Dynamics of solitons in polyacetylene with interchain coupling

Geraldo Magela e Silva
Departamento de Fisica, Universidade de Brasilia, 70910 Brasilia, Distrito Federal, Brazil

Akira Terai
Department of Physics, University of Tokyo, Bunkyo-Ku, Tokyo 113, Japan
(Received 19 November 1992)

The interchain charge transfer and interactions of two chains are studied numerically through the dynamics of charged and neutral solitons in the presence of an electric field by using the Su-Schrieffer-Heeger model. The electric field is introduced in terms of a time-dependent vector potential which is included in the Hamiltonian through a Peierls substitution of the phase factor to the transfer integral. The effects of confinement on the soliton motion are determined. In particular, the viability of a single moving soliton to cross an interacting region between two parallel chains is analyzed, and its relationship to soliton velocity and interaction region extent is determined. The interchain charge-transfer probability is considered. The charge-transfer probability in a collision between a charged and a neutral soliton belonging to neighboring chains is determined. It is shown that a pair of solitons, one on each chain, can move freely together in an oscillatory way, without any confinement. The oscillation frequency is estimated and its relationship to experimental data is clarified.

I. INTRODUCTION

The proper understanding of the mechanisms of charge conduction in *trans*-polyacetylene has attracted considerable attention in the last decade. This interest, in both the theoretical and experimental fields, is justified by the nature of this material. Besides exhibiting a metallic conductivity under certain doping concentrations, it has a very simple structure. The initial step towards the understanding of the theoretical aspects of trans-polyacetylene was taken by Su, Schrieffer, and Heeger (SSH),[1,2] in their construction of the most-used model of this conjugated polymer. After that, several authors have enhanced our knowledge about polyacetylene by considering other aspects not treated directly by the SSH model as well as by adding to the model, e.g., Refs. 3–8.

Recently, authors have been concerned with dynamic aspects involved in the study of trans-polyacetylene, especially those aspects related to the presence of solitons.[4,5] Also the so-called higher-dimensional problem has received attention, since the real material exhibits three-dimensional conduction.[6–10] It is the purpose of this work to present a dynamic study involving the higher-dimensional characteristics of trans-polyacetylene using an enhanced version of the SSH model.

Since moving solitons are expected to play a major role in the conduction process in polyacetylene, we perform two types of studies, the first one involving a single soliton and the second involving a pair of solitons. In the first study we consider two neighboring chains interacting with each other, one of them containing a moving soliton. In our simulations, we treat those situations that seem to contain the most important effects. The cases where we consider a single soliton are shown schematically in Fig. 1. In the first case, two neighboring chains without solitons are allowed to interact in the central region. In the second case, a charged soliton moving on chain 1 "collides" with the small region where there exists interaction between the two chains. The third case deals with a collision with a quite extensive interaction region.

In the second study, we are concerned with the interaction of two solitons on neighboring chains (Fig. 2). We consider a moving charged soliton interacting with an initially static neutral soliton. We study three distinct representative cases. First, one charged soliton trapped by the impurity is depinned and put into motion through the electric field. Then it penetrates a coupled region between the chains. Close to this interacting region, on the neighboring chain, sits a second and neutral soliton. In the second case, two neighboring chains interact throughout their extent, each one bearing one soliton in a corresponding soliton position. One chain bears a trapped charged soliton and the other bears a neutral soliton. The system is subjected to an electric field. In the third case the same system as in the second case is subjected to an electric field of greater absolute value. Charge transfer as well as confinement potentials are analyzed in the various situations.

These systems, where the charged solitons begin to move under the action of an electric field, are studied by numerically solving the coupled equations of motion for the lattice displacements and the electronic wave functions. These equations are numerically integrated over real time. As for the model, we use SSH-type Hamiltonians for each chain, which are modified to include the electric field, an interchain coupling term, and an impurity potential. The impurity potential is a necessary device to concentrate the extra charge of the system on a single soliton. We use a short-ranged site-type impurity that locally varies the site energy of the π electron.

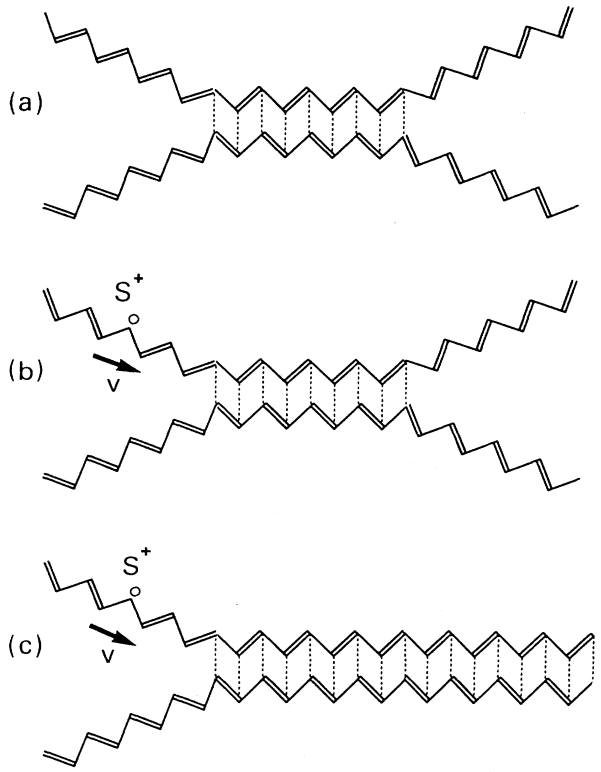

FIG. 1. Schematic representation of the single-soliton study. (a) Two polyacetylene chains interacting only in the central sites without any soliton; (b) two chains interacting only in the central sites with an incoming soliton; (c) two chains interacting in all the sites from the middle to the right with an incoming soliton.

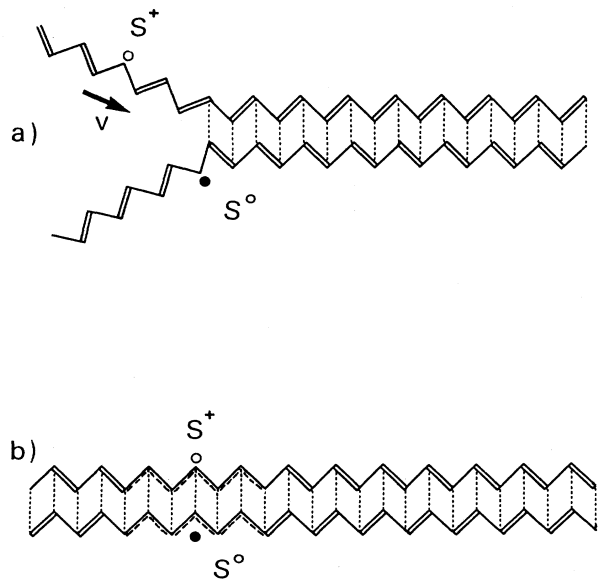

FIG. 2. The second study—neighboring polyacetylene chains bearing one soliton each. (a) Two chains interacting in all the sites from the middle to the right with an incoming charged soliton; (b) two chains interacting along all their sites, with the solitons occupying correspondent positions initially.

The acceptor-doping case is studied, where the sign of the impurity potential is positive and its absolute value very small, its presence being noted only in the initial state. Since we consider a uniform electric field, the time-dependent vector potential is independent of the space coordinate, then the periodic boundary condition can be adopted to avoid edge effects. The initial static states are obtained by iteratively solving a coupled set of self-consistent equations.[11]

The time evolution of the electron-density distribution, bond configurations, soliton positions, soliton velocities, and involved energies are explicitly showed.

The organization of this work is as follows. In Sec. II the model Hamiltonian and the outline of the method of numerical simulation are described. In Secs. III and IV the results of the simulations are shown. Finally, in Sec. V a summary and discussions are presented.

II. MODEL AND FORMALISM

In this study we use the following Hamiltonian to describe the system:

$$H = H_1 + H_2 + H_{\rm int}, \tag{1}$$

$$H_j = -\sum_{n,s}(t_{j_n,n+1}C^{\dagger}_{j_{n+1},s}C_{j_n,s} + \text{H.c.}) + \sum_n \frac{K}{2}(u_{j_{n+1}} - u_{j_n})^2 + \sum_n \frac{M}{2}\dot{u}^2_{j_n}, \tag{2}$$

with

$$t_{j_n,n+1} = e^{+i\gamma A}[t_0 - \alpha(u_{j_{n+1}} - u_{j_n})], \quad j = 1,2$$

and

$$H_{\rm int} = -\sum_{s,n=p}^{q} t_{\perp}(C^{\dagger}_{1_{n,s}}C_{2_{n,s}} + C^{\dagger}_{2_{n,s}}C_{1_{n,s}}) + \sum_s V(C^{\dagger}_{1_{m,s}}C_{1_{m,s}} + C^{\dagger}_{1_{m+1,s}}C_{1_{m+1,s}}). \tag{3}$$

Here H_1 and H_2 are SSH-type Hamiltonians, modified to include the electric field. $C_{j_n,s}$ is the annihilation operator of a π electron with spin s on the j chain at the nth lattice site, u_{j_n} is the displacement coordinate of the nth CH group on chain j, t_0 is the transfer integral between the nearest-neighbor sites in the undimerized chains, α is the electron-phonon coupling, M is the mass of a CH group, K is the spring constant of a σ bond, $t_{\perp}$ is the transfer integral between sites with the same index on different chains from p site to q site, and V is the strength of an impurity which is located between the mth and the $(m+1)$th sites (when we have two solitons in the system, V is a necessary device to concentrate initially the charge in a given soliton). $\gamma \equiv ea/(\hbar c)$, e being the absolute value of the electronic charge, a the lattice constant, and c the light velocity. The relation between the time-dependent vector potential A and the uniform electric

field E is given by $E = -\frac{1}{c}\dot{A}$.

First, we prepare a stationary state, which is fully self-consistent with respect to both degrees of freedom, of the electrons and phonons, as the initial conditions of the calculations.[11] Then, under the action of the electric field, the electronic and the lattice equations of motion are numerically integrated, namely, the time-dependent Schrödinger equation,

$$i\hbar\dot{\Psi}_{j_{k,s}}(n,t) = -t_{j_{n,n+1}}\Psi_{j_{k,s}}(n+1,t) - t^{*}_{j_{n-1,n}}\Psi_{j_{k,s}}(n-1,t) - \begin{cases} 0 & \text{for } n<p,\ n>q \\ t_{\perp}\Psi_{\hat{j}_{k,s}}(n,t) & \text{for } p\le n\le q \end{cases} + V\delta_{n,m}\delta_{j,1}[\Psi_{j_{k,s}}(m,t) + \Psi_{j_{k,s}}(m+1,t)], \tag{4}$$

where j and $\hat{j}$ are chain indices ($\hat{j}$ = 2,1 for j = 1,2, respectively) and k is the quantum number which specifies an electronic state; and the lattice equation of motion

$$M\ddot{u}_n = F_n(t), \tag{5}$$

where

$$\begin{aligned} F_n(t) = &-K[2u_n(t) - u_{n+1}(t) - u_{n-1}(t)] \\ &+\alpha[e^{i\gamma A(t)}(B_{n,n+1} - B_{n-1,n}) \\ &+e^{-i\gamma A(t)}(B_{n+1,n} - B_{n,n-1})]. \end{aligned} \tag{6}$$

Here $B_{n,n'} \equiv \sum'_{k,s}\Psi^{*}_{k,s}(n,t)\Psi_{k,s}(n',t)$. Since the equations of motion for u_1 and u_2 have the same form, we have dropped the index characterizing the chain in the above equation. The prime on the summation means that the sum is taken over the occupied states in the initial stationary state. These equations of motion are solved by discretizing the time variable with a step Δt. The time step Δt is chosen so that the change of $u_n(t)$ and $A(t)$ during this interval is always very small in the electronic scale. The time-dependent Schrödinger equation is analytically integrated by introducing single-electron eigenstates at each moment. We have that

$$\Psi_k(t) = T\exp\left(-i\int_0^t dt'\frac{\hat{h}(t')}{\hbar}\right)\Psi_k(0),$$

where $\hat{h}(t')$ is the electronic part of the Hamiltonian $H(t)$ at time t'. Discretizing the time, this expression becomes

$$\Psi_k(t_{j+1}) = \exp\left(-i\Delta t\frac{\hat{h}(t_j)}{\hbar}\right)\Psi_k(t_j).$$

Introducing the expansion,

$$\Psi_k(t_j) = \sum_l C_{lk}\phi_l(t_j),$$

where $C_{lk} = \langle\phi_l|\Psi_k\rangle$, and $\{\phi_l\}$ and $\{\varepsilon_l\}$ are the eigenfunctions and the eigenvalues of the electronic part of the Hamiltonian $H(t)$ at a given time t_j. The solution of the time-dependent Schrödinger equation can then be put in the form,

$$\Psi_{k,s}(n,t_{j+1}) = \sum_l\left[\sum_m \phi^{*}_{l,s}(m,t_j)\Psi_{k,s}(m,t_j)\right] \times\exp\left(-i\frac{\varepsilon_l\Delta t}{\hbar}\right)\phi_{l,s}(n,t_j). \tag{7}$$

The lattice equations are written as

$$u_n(t_{j+1}) = u_n(t_j) + \dot{u}_n(t_j)\Delta t, \tag{8}$$

$$\dot{u}_n(t_{j+1}) = \dot{u}_n(t_j) + \frac{F(t_j)}{M}\Delta t. \tag{9}$$

Therefore, using Eqs. 7–9, the electronic wave functions and the displacement coordinates at the $(j+1)$th time step are obtained from the jth time step.

We use as parameters the commonly accepted values for polyacetylene: t_0 = 2.5 eV, $t_{\perp}$ = 0.075 eV, K = 21 eV Å^{-2}, α = 4.1 eV Å^{-1}, and a = 1.22 Å, and for the impurity potential we take V = 0 in the single-soliton study. In the double-soliton study we take V = 0.0025 eV, which is large enough to concentrate the charge in the trapped charged soliton ($\approx$ 99%), and considerably small to not influence significantly the system after the depinning of the soliton.[5] Periodic boundary conditions are assumed for the electronic wave functions $\Psi_{k,s}$ and the lattice displacements u_n.

In the single-soliton study, the total number of lattice points on chain 1 (N_1) and on chain 2 (N_2) are as follows: N_1 = 100 in the first case, where there is no soliton present, and N_1 = 101 in the second and third cases, where there is a soliton on chain 1. N_2 = 100 in all studied cases, where there exist no solitons on chain 2. The total number of electrons on each chain (Ne_1, Ne_2) are given by $Ne_1 = Ne_2$ = 100 in all cases, which means that in the initial condition we have a positively charged soliton on chain 1 in the second and third cases.

In the double-soliton study, the total number of lattice points on each chain are $N_1 = N_2$ = 101. The total number of electrons on each chain (Ne_1, Ne_2) are Ne_1 = 100 and Ne_2 = 101. Hence, we have two interacting chains each bearing 101 sites. Each chain bears a single soliton. Chain 1 bears a positively charged soliton and chain 2 a neutral one.

To study the position of the soliton as a function of time, we introduce a smoothed bond variable by

$$\overline{y}_n = \frac{(-1)^n}{4}(y_{n-1} - 2y_n + y_{n+1}),$$

with $y_n \equiv u_{n+1} - u_n$. When there is a single soliton, $\overline{y}_n$ has a tanh-like form. Thus its difference $\overline{y}_{n+1} - \overline{y}_n$ has a sech-like form. Since we consider the periodic system in the present simulation, it is convenient to define the soliton position by[4]

$$x(t) = \frac{Na}{2\pi}\arg\left\{\sum_{n=1}^{N}\exp\left(\frac{(2n+1)\pi i}{N}\right)(\overline{y}_{n+1} - \overline{y}_n)\right\}. \tag{10}$$

We observe the position at every 100 time steps. The velocity of the soliton is approximated by the difference of the position in the following form:

$$v(t + 50\Delta t) = \frac{x(t + 100\Delta t) - x(t)}{100\Delta t}.$$

A time step of $\Delta t = 0.01\omega_Q^{-1} = 0.04$ fs is used. We follow the dynamics of the systems up to the 12 900th time step in the single-soliton study and in the first case of the double-soliton study. In the second and third cases of the double-soliton study we follow it up to the 25 000th time step. These simulations take 2 and 4 h, respectively, of CPU time on a supercomputer HITAC S-820.

III. SIMULATION RESULTS—SINGLE SOLITON

In the first simulation, we have considered two parallel chains without solitons. We take $N_1 = N_2 = Ne_1 = Ne_2 = 100$. The two chains are allowed to interact only in the ten central sites, i.e., $p = 46$ and $q = 55$ [Fig. 1(a)]. Then we have calculated the stationary state for the two possible configurations: the in-phase and the out-of-phase arrangement of the double bonds.

We have obtained that the out-of-phase arrangement is energetically preferred, as should be expected with this sort of interchain interaction.[8] Also, our calculated value for the confinement energy, $\Delta E = 2.36 \times 10^{-3} t_0$, is in perfect agreement with the analytical value obtained by Baeriswyl and Maki, Ref. 8, given by the following relation: $\Delta E(l) = 2t_\perp^2 l/(\pi v_F)$, where $l \equiv (q-p)a$ in the present work.

We have then considered the possibility of a moving soliton passing across an interacting region between the chains, where the chains are initially in the out-of-phase state. Since a moving soliton leaves behind a reordering of the dimerization pattern, as soon as the soliton enters the interacting region, the potential energy of the chains will increase, with a consequent decrease in the soliton kinetic energy. To analyze in detail this process, we have considered two different ranges of interchain coupling [see Figs. 1(b) and 1(c)]. As can be seen in Fig. 1(b), first we have considered the "collision" of the charged moving soliton with a small interchain interaction region ($q-p = 10$), and then, Fig. 1(c), a collision with a much larger region ($q - p = 50$).

As the initial state in all cases represents a stationary solution, we make the charged solitons start to move through the application of the electric field on the system. The electric field is applied from $t = 0$ to $t = t_{\rm off}$, a time span necessary for the charged soliton to acquire a velocity close to its maximum possible value.[4] To do that, we put $A = -cEt$ from $t = 0$ up to $t = t_{\rm off}$, and then, for times greater than $t_{\rm off}$, we set $A = -cEt_{\rm off}$. We take $t_{\rm off} = 17\omega_Q^{-1}$ and $|E| = 0.025E_0$, with $E_0 = \hbar\omega_Q/(ea)$.

In Fig. 3 we show the snapshots of the smoothed bond variable $\overline{y}_n$. Figure 4 gives the time dependence of the soliton position.

In the collision with the shorter region, the soliton passes through it, but with a consequent decrease on its velocity. This is because after the soliton leaves the interaction region, the double bonds are in the less stable in-phase configuration.

When the soliton collides with the larger region, its kinetic energy decreases continuously until the soliton velocity eventually vanishes. Then, it starts moving again in the contrary direction to the former motion. In short, the soliton is reflected in the "shock" with the larger interacting region, cf. Fig. 4. The lattice kinetic energy does not vanish even when the soliton stops. This nonzero energy comes mainly from phonons left behind the soliton (see Fig. 3). In Fig. 4, the soliton position

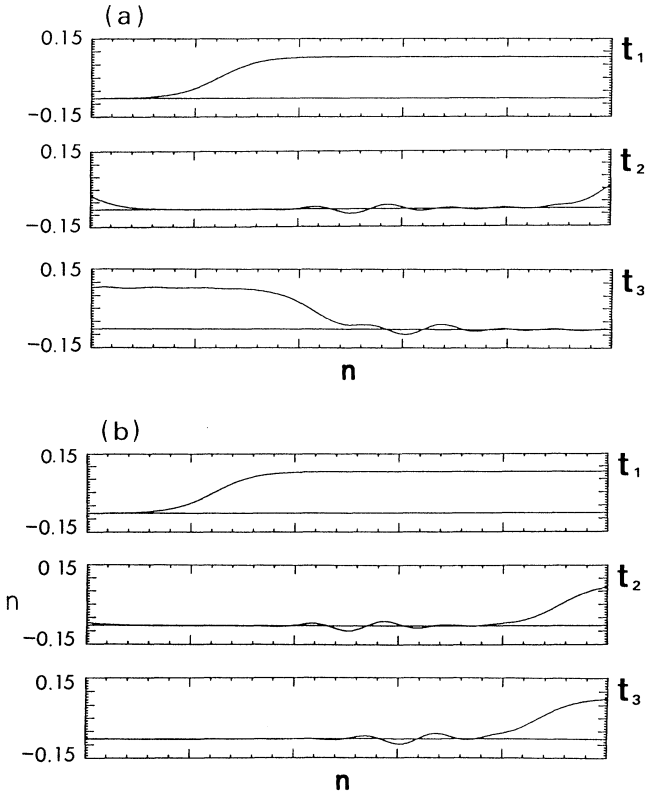

FIG. 3. Diagrams of the smoothed bond configuration $\overline{y}_n = (-)^n(y_{n-1} - 2y_n + y_{n+1})/4$; (a) two chains of 101 sites interacting only in the 10 central sites, (b) two chains of 101 sites interacting in the 50 sites from the middle to the right. $t_1 = 0\Delta t$, $t_2 = 6000\Delta t$, $t_3 = 10\,000\Delta t$. $\Delta t = 0.04$ fs. Boundary conditions are such that $\overline{y}_1 = -\overline{y}_{N+1}$. The ordinate is $\overline{y}_n$ in Å.

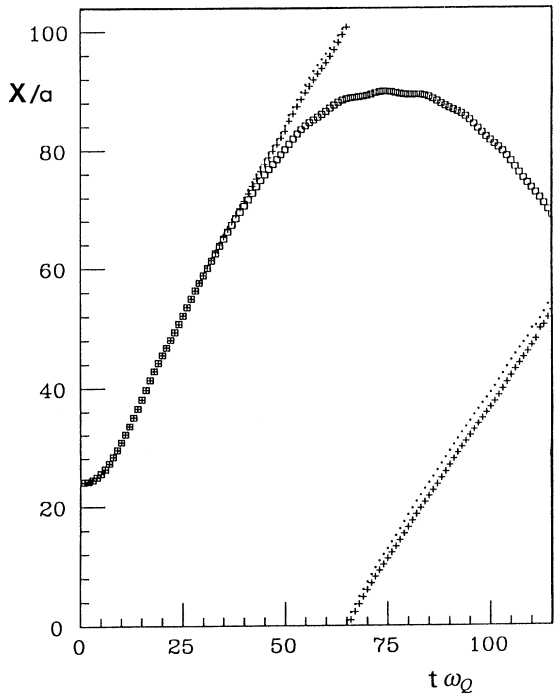

FIG. 4. Time evolution of the soliton position. Dots, no interacting chains; crosses, chains interacting in the ten middle sites only; squares, chains interacting in the 50 sites from the middle to the right.

versus time, we can identify a parabolic behavior. The soliton is uniformly decelerated. This is because the confinement energy is a linear function of l, where l is the size of the in-phase region. Let us estimate the effective mass of the soliton. For this purpose, we have fitted the data of the soliton position to $x(t) = a_0 + a_1 t - \frac{1}{2}a_2 t^2$. The resulting value of a_2 is $0.0286 a\omega_Q^2$. Since the confinement energy is $(t_\perp^2/\pi t_0)l$, the effective mass is estimated by

$$m = \frac{t_\perp^2}{\pi t_0 a_2}.$$

The resulting value of m is $4.7 m_e$, where m_e is the free-electron mass. The soliton position can also be determined from the charge distribution using a formula analogous to Eq. (10). In this case, we obtain $a_2 = 0.0308 a\omega_Q^2$ and $m = 4.4 m_e$. The reason for the difference in these two estimations is unknown at the present stage. However, these values are in good agreement with another estimation obtained from the dependence of the total and lattice kinetic energies on the soliton velocity.[12]

Next we discuss the time dependence of the various energies involved in the process. Let us define the electronic energy E_e, the lattice potential energy $E_{\rm LP}$, the kinetic energy of the lattice E_{LK}, and the total energy E_T by

$$E_e(t) = \sum_{k,s}{}' \sum_{l,j} \varepsilon_l \left[\sum_n \phi^*_{j_{l,s}}(n,t) \Psi_{j_{k,s}}(n,t) \right]^2, \tag{11}$$

$$E_{\rm LP}(t) = \frac{K}{2} \sum_{n,j} [u_{j_{n+1}}(t) - u_{j_n}(t)]^2, \tag{12}$$

$$E_{LK}(t) = \frac{M}{2} \sum_{n,j} \dot{u}^2_{j_n}(t), \tag{13}$$

and

$$E_T(t) = E_e(t) + E_{\rm LP}(t) + E_{LK}(t). \tag{14}$$

We observe that the electronic and lattice potential energies present a rapidly oscillatory behavior enveloped by more general features related to the actual state of the soliton. The mean electronic energy increases after the soliton enters the interaction region. This increase is enhanced when the soliton velocity slows down. The lattice potential energy has a behavior analogous to $E_e(t)$, but with an inverse dependence on the soliton velocity. The rapid oscillation is not due to the interchain interactions. To confirm this fact, we have made a similar numerical calculation in a system without interactions. A similar oscillation is clearly seen. This oscillation, most probably, comes from the shape mode, which is one of the phonon modes localized around the soliton.[13,14]

The total energy increases rapidly during the application of the electric field, as should be expected. After the field is switched off, the total energy becomes constant. A small variation of the total energy is observed over the time; it is thought to come from the discretization of the time variable. Since this variation is small enough, it is verified that the mesh adopted for the time variable is quite good. The total energy remains constant even after some charge transfer taken place.

Finally we discuss the charge transfer that takes place when the charged soliton enters the interacting regions. Figure 5 shows the time dependence of the expectation value of the total hole charge in chain 1,

$$Q(t) = \sum_{n=1}^{N_1} \left[1 - \sum_{k,s}{}' \Psi^*_{1_{k,s}}(n,t) \Psi_{1_{k,s}}(n,t) \right].$$

The total amount of the charge transferred from chain 1 to chain 2 is $1 - Q(t)$.[15] In the first case, where there is no interchain interaction, obviously there is no charge transfer also, as can be seen by the straight line that remains unity all the time. The second case presents two valleys at the time steps corresponding to the shocks of the soliton with the interacting region. The second shock takes place because of the boundary conditions adopted, i.e., after the first shock, the soliton continues to move until it reaches the end of its chain, then it reappears at the beginning and goes to the second shock. From the third case, we obtain the most interesting aspects of the charge transfer involved in these situations. It is observed that the charge transfer takes place only when the soliton enters the interacting region. The total amount of the transferred charge shows a plateau while the soliton is moving in the coupled region, although a slight decrease is seen when the soliton stops. The charge-transfer

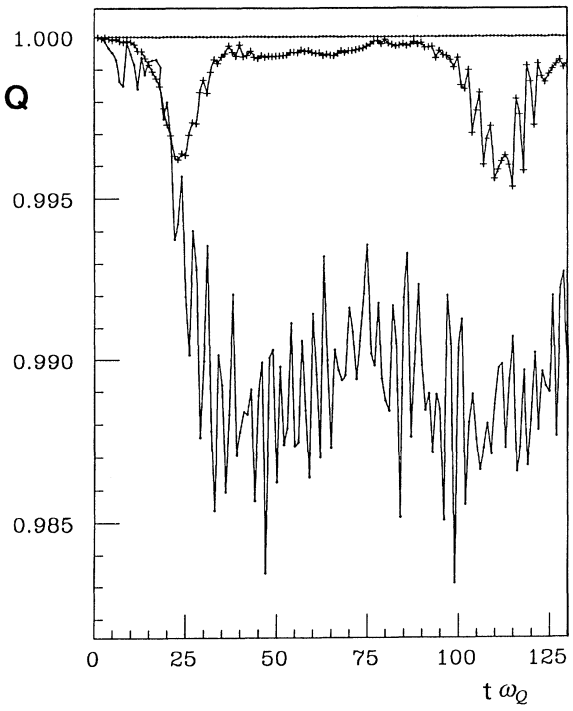

FIG. 5. Charge-transfer time dependence. Straight dotted line, no interacting chains; crosses, chains interacting in the ten middle sites only; dots, chains interacting in the 50 sites from the middle to the right.

probability oscillates as a function of time. This oscillation may be mainly due to the quasiresonance between the mid-gap state in chain 1 and the valence-band states in chain 2. From these pictures we can observe that no charge transfer occurs when the soliton completely leaves the interacting region.[16] Therefore, although the two chains are interacting all the time, it is the presence or not of the soliton as well as the length of the interacting region that definitively determine the paths of charge conduction.

IV. SOLITON PAIR

We perform simulations in three important representative cases. In Fig. 2 we depict in two diagrams the aspects of the initial conditions adopted in the calculations. Figure 2(a) represents the first situation, where two neighboring chains are coupled over half their length, from the central region to the right (p=51 and q=94). In chain 1 there exists an initially stationary positively charged soliton, relatively far from the coupling region (site number 20). In chain 2, a stationary neutral antisoliton sits very close to the interacting region (site number 45).

Figure 2(b) shows two parallel neighboring chains. These two chains are allowed to interact with each other along all their extension (p=1 and q=101). Initially, as represented in the figure, a stationary positively charged soliton sits on chain 1. On chain 2, a stationary neutral antisoliton remains in a site corresponding to the position of the charged soliton in chain 1 (site number 20). In this way, with the two solitons occupying the same position in the corresponding chains, we obtain a stable solution that can be used as the initial condition. With the configuration of Fig. 2(b) we carry out two different calculations through the application of electric fields of different intensities.

After the settlement of the initial conditions, we proceed with the simulation through the application of the electric field on the systems. Figure 6 shows the time evolution of the solitons in the first case [Fig. 2(a)]. We follow the dynamics of the system up to the 12 900th time step. The electric field is applied in the first 1500 time steps, the electric-field strength being $|E| = 0.025E_0$. This short-time application of the electric field is a convenient device utilized to give velocity to the initially stationary charged soliton. The moving charged soliton then comes to interact with the neutral soliton and the coupled region.

In its motion, the charged soliton passes the neutral soliton and enters deeply in the coupled region. Then, the charged soliton velocity slows down, decreasing continuously until it vanishes completely. Simultaneously, the neutral soliton is pulled into the coupled region ac-

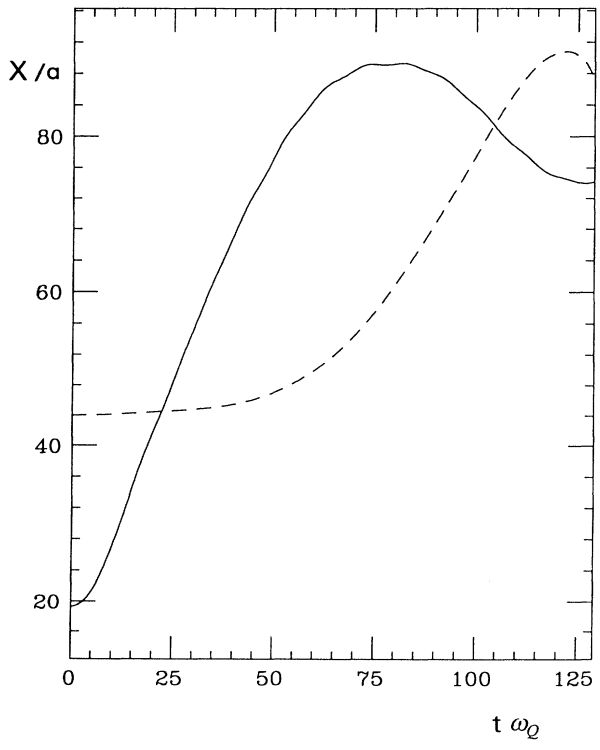

FIG. 6. Time evolution of the soliton positions corresponding to the initial configuration represented in Fig. 2(a). Solid line, charged soliton; dashed line, neutral soliton.

celerating once it enters there. The charged soliton reverses direction, colliding with the incoming neutral soliton. After the collision, the two solitons separate from each other. As the distance between them increases, their respective velocities decrease. The solitons then stop and again reverse direction, colliding once again.

Figure 7 shows the time evolution of the solitons' positions in the second and third cases [Fig. 2(b)]. These two cases have the same initial conditions. Nevertheless, the intensity of the applied electric fields is different in each case in order to observe features independent of the electric-field strength. We follow the dynamics of the system up to 25 000 time steps. As in the previous case, a constant electric field is applied in the first 1500 time steps. We use the following values to the electric fields: $|E_1| = 0.025E_0$ and $|E_2| = 0.015E_0$. These two simulations present the same basic pattern. The charged soliton in chain 1 is accelerated and put into motion by the electric field initially applied to the system. As the charged soliton proceeds in its motion the neutral soliton is pulled in the direction of the charged soliton. The charged soliton velocity decreases continuously, vanishes, and then begins to increase in the opposite direction. The two solitons collide. After the collision, the solitons separate a few sites from each other, their velocities decrease, vanish, and restart to increase in the opposite direction and then a new collision occurs. This oscillatory behavior continues through the simulation with the frequency of collisions almost constant in time and with a decrease in the amplitude of separation of the solitons between the collisions. Naturally, the amplitudes are greater with E_1, where the stronger electric field induces more velocity to the charged soliton.

The time dependence of the lattice kinetic energy involved in the various cases is depicted in Fig. 8. This energy increases rapidly during application of the electric field when the charged soliton acquires considerable velocity. When the electric field is removed the kinetic energy decreases to a lower plateau and begins to oscillate accompanying the interaction of the solitons. This oscillation presents peaks corresponding to each soliton collision. At a collision, the two solitons are moving fast and in opposite directions. The valleys correspond to instances where the solitons are stopped or moving very slowly. Note that the kinetic energy does not vanish even when the two solitons are stopped. This nonzero energy is due to phonons left behind the soliton.

The electronic and lattice potential energies have a

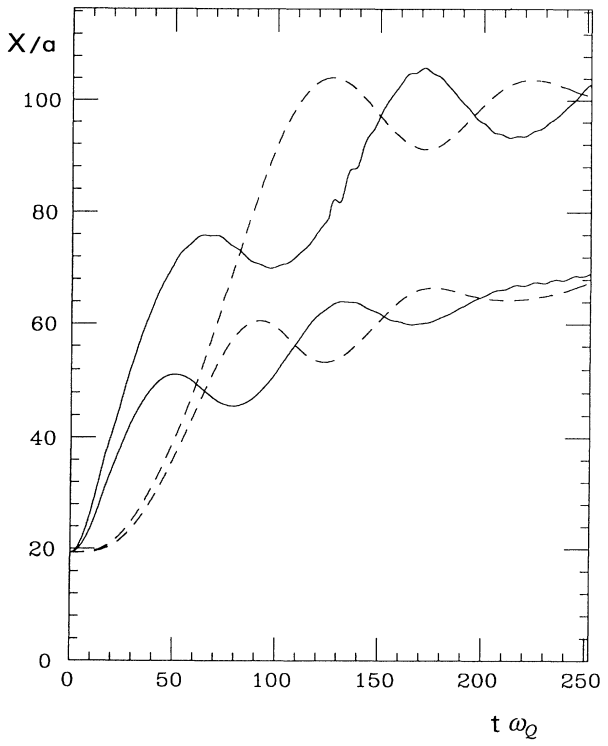

FIG. 7. Time evolution of the soliton positions corresponding to Fig. 2(b). Solid lines are for the charged solitons and dashed lines for the neutral ones. The upper lines correspond to the stronger electric field and the bottom lines to the weaker electric field.

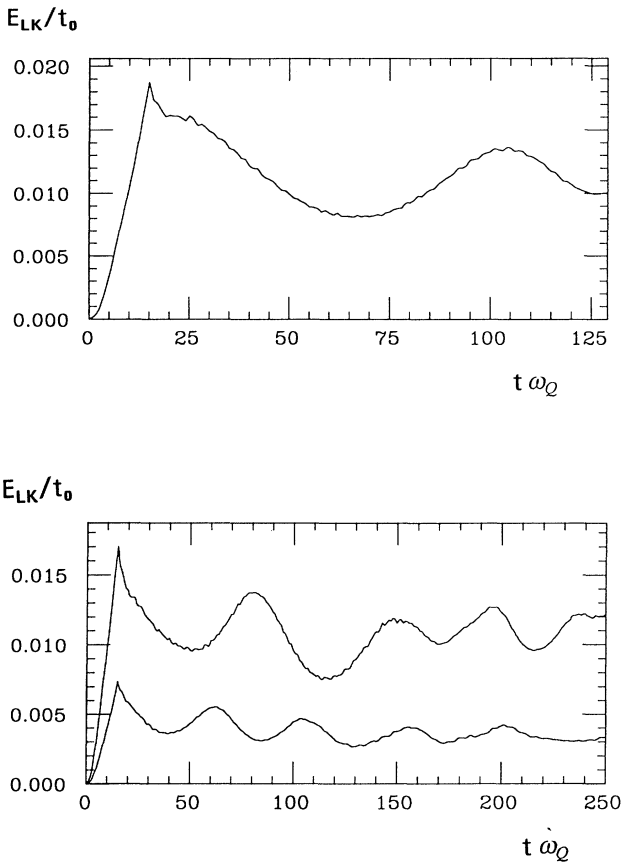

FIG. 8. Time dependence of the lattice kinetic energy. (a) corresponds to Fig. 2(a); (b) corresponds to Fig. 2(b), the upper line correspond to the stronger electric field and the lower line to the weaker field.

rapid oscillatory motion enveloped by a slow oscillation. The fast oscillation is thought to come from the shape mode, which is one of the phonon modes localized around the soliton.[14] The slow oscillation is directly related to the soliton motion. The electronic energy variation becomes negative when the electric field is applied to the system and the solitons start to move. Then it increases or decreases as the solitons are stopping or moving, respectively. Therefore, there are peaks of the slow oscillation when the solitons both are moving slowly, and valleys when they are colliding and moving fast. The lattice potential-energy variation is positive almost all the time and presents a behavior analogous to the electronic energy variation but with an inverse dependence on the soliton velocities.

The charge transfer involved in the various analyzed situations is depicted in Fig. 9. There, we show the time dependence of the expectation value of the total hole charge in chain 1, $Q(t)$. Figure 9(a) presents the charge transfer in the first case, i.e., the two chains interacting through half their length. We can observe that some charge transfer takes place only when the charged soliton enters the coupled region and when there is a collision between the solitons. With the two solitons very far from each other, the total amount of transferred charge shows a plateau. Figures 9(b) and 9(c) show the second and third cases, respectively. The two chains are allowed to interact all over their length; therefore we can focus on the influence of the intersoliton distance on the charge transfer. We can observe clearly that the amount of transferred charge is enhanced when the solitons collide with each other and that this amount is lessened when the solitons are far from each other, decreasing with the distance. In Fig. 9(b) some charge returns to the charged soliton around $t = 180\omega_Q^{-1}$. This episode is thought to be spurious and its reason is unknown at present. All the cases present small oscillations as a function of time that may be mainly due to the quasiresonance between the midgap states of chains 1 and 2.

Figure 10 shows the time evolution of the midgap levels of the solitons. Although the scale of the variation is very small, some insight can be gained by its analysis. We find that initially the charged soliton is pinned by the impurity. After the depinning, caused by the electric-field application, the midgap level corresponding to the charged soliton tends to join the midgap level of the neutral soliton. When the external electric field is switched off the two levels oscillate over time with level crossings corresponding exactly to each collision of the solitons. The levels split apart from each other when the solitons are distant one from another. This behavior, successive

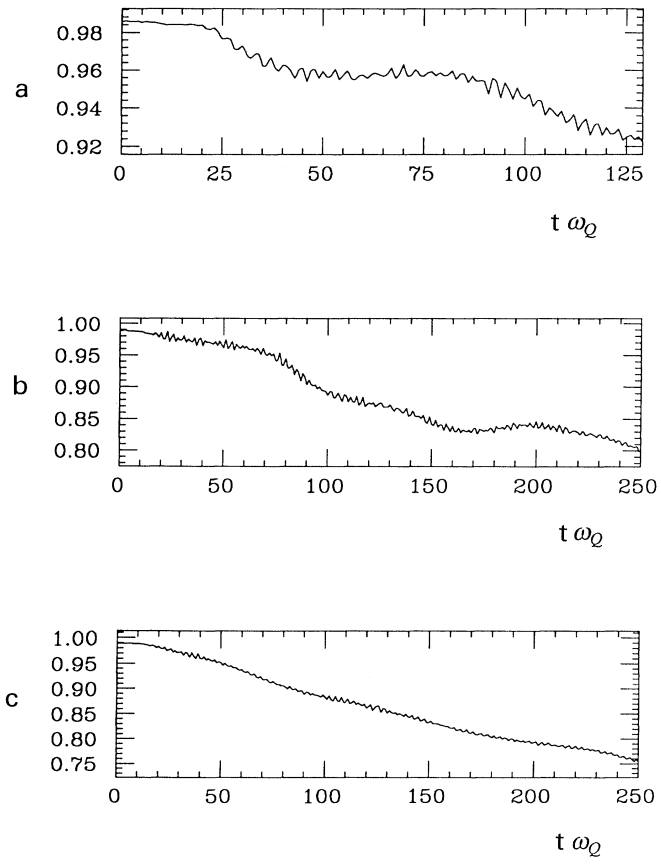

FIG. 9. Time dependence of the charge transfer. (a) corresponds to Fig. 2(a); (b) corresponds to Fig. 2(b), with the stronger electric field; (c) corresponds to Fig. 2(b) with the weaker electric field. The ordinate represents the positive charge on the charged soliton in units of $+e$.

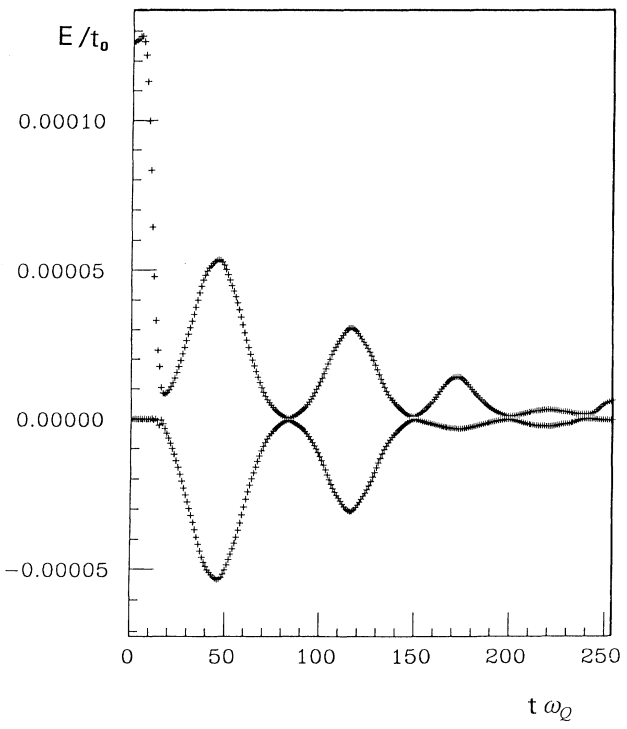

FIG. 10. The midgap levels as functions of time for the case of Fig. 2(b) with the stronger electric field.

splitting and crossings of levels, can account for the enhancement of charge transfer at the soliton collisions.

V. DISCUSSION AND SUMMARY

The interchain interaction and charge transfer of two polyacetylene chains, interacting through hopping terms and the concurrent effects of moving solitons, have been investigated. This study was carried out through numerical calculations using an improved version of the SSH model to accommodate the more complex aspects involved in the actual system. We have used an electric field to put a charged soliton in motion. The electric field is introduced in the model Hamiltonian as a time-dependent vector potential in the phase of the transfer integral. The time-dependent Schrödinger equation and the equation of motion for the time-dependent lattice displacements form a coupled set that was numerically integrated over the time in a self-consistent way.

The calculations are conducted from first principles without any previous assumption on the form of the moving solitons.

The adopted model for the coupling between the chains has the advantage of being quite simple and able to reproduce the principal features of soliton confinement. Nevertheless, as revealed by some authors,[6,7] this type of coupling determines an out of phase (antiparallel) relative order of the dimerization pattern, in contrast with the experimentally observed in-phase (parallel) alignment of the dimerization.[17]

The stationary state of two chains interacting along ten parallel sites is numerically calculated with the dimerization pattern out of phase and with it in phase. The difference in energy of the two possible relative orders of alignment is perfectly in accordance with the analytical result of Ref. 8.

The ability of a soliton to actually pass through an interacting region between two neighboring chains has been investigated in two enlightening situations. An initially static charged soliton is accelerated through the application of an electric field until it reaches a velocity close to its maximum possible velocity.[4] Then the electric field is switched off and the soliton continues to move until it eventually reaches an interacting region.

When the interchain interaction is restricted to only ten sites, we have observed that the soliton, which possessed a considerable kinetic energy, could pass across this small interaction region. Since the resulting configuration of the dimerization bonds has become less stable after the soliton passage (there has been an increase in the sum of the lattice potential and electronic energies) the soliton kinetic energy is decreased and the soliton velocity is slowed down. We have considered periodic boundary conditions, then as the soliton has passed through the interacting sites, it has made a round trip and returned to the interchain interacting place, which was now on in-phase configuration. On this second collision, the soliton has recomposed the more stable configuration of the chains and has increased its kinetic energy in doing so, as should be expected.

With a much larger interacting region, with 50 interacting sites, we have observed the interesting effect of soliton reflection. The charged moving soliton has collided with this long interacting region in a quasielastic fashion. As it has entered the interacting place, its velocity slowed down and its kinetic energy became lower and lower, until the soliton stopped and started moving again in the contrary direction. From the resulting parabola drawn in the graph of the soliton position versus time, we have estimated an effective force acting upon a soliton as it enters a region where two chains are allowed to interact.

The calculations of the charge transfer have revealed that the probability of charge transfer between a chain having a charged soliton and a chain without it is quite small. One should expect that, since the gap between the midgap state and the band states is large enough to prevent hopping.

For the study involving two solitons belonging to neighboring chains, in the various situations that we have considered, there was a drift of the neutral soliton caused by the moving charged soliton. This drift is a result of the confinement potential that links the solitons. Namely, the two solitons are attracted to each other to avoid the matching of the double bonds between the chains and the resulting increase on the sum of the lattice potential and electronic energies. Therefore, we observe that the mobility of solitons in coupled polyacetylene chains is possible only as a collective phenomenon involving other solitons on neighboring chains. Otherwise, the confinement potential will make the moving soliton recoil or simply oscillate.

We define a collision as the time when a soliton on one chain is at the opposite site from a soliton on another chain. After each collision an inner effective force between the solitons pulls them back against each other. When a moving soliton collides with a stationary soliton, the pair of solitons move together with a change between the solitons in the head position. The frequency of this oscillation has a well-defined value that is independent of the initial velocity of the former moving soliton. In all studied cases the period between two successive collisions is about $45\omega_Q^{-1}$, which corresponds to an angular frequency of $0.14\omega_Q = 0.035$ fs^{-1}. We think that this oscillation between solitons may be the source of some peaks observed on infrared-absorption spectra.[18]

Charge transfer takes place between the charged and the neutral soliton when they are close enough. When the distance between the solitons is about $15a$ or closer, the charge transfer is enhanced because at this distance the midgap states start to overlap. An amount of charge of about 5% is transferred from the charged to the neutral soliton after each collision.

The midgap levels undergo an oscillation that also accompany the oscillatory motion of the solitons. The two levels get very close and even touch each other at the soliton collisions and then split and separate when the solitons are far from each other. Coincident with the level touching there is an enhancement in the charge transfer. However, we stress that the splitting is very small, the overlap of the two levels also is small (the soliton state on one chain is mostly different from zero on odd

sites while the soliton state on the other chain is mostly different from zero on even sites), and we have moving solitons which have different wave functions from those of the static solitons.[19]

The treatment dispensed here to the interchain coupling between the polyacetylene chains is considered to be satisfactory to observe several of the aspects involved in the interchain interaction. Nevertheless, a more realistic interchain coupling could furnish new and more accurate information about the interchain charge-transfer mechanisms involved in conjugated polymers. It is the purpose of a forthcoming paper to present detailed studies, with more realistic coupling terms, of the mechanisms of confinement of solitons and interchain charge transfer using the present formulation as the theoretical start point.

ACKNOWLEDGMENTS

The authors would like to express sincere gratitude to Professor Y. Wada and Professor Y. Ono for encouraging discussions. This work was partly supported by a Grant-in Aid for Scientific Research from the Ministry of Education, Science and Culture, Japan. Numerical calculations were performed on a HITAC S-820 supercomputer of the computer center of the Institute for Molecular Science, Okasaki National Research Institutes.

[1]W. P. Su, J. R. Schrieffer, and A. J. Heeger, Phys. Rev. B **22**, 2099 (1980); **28**, 1138(E) (1983).
[2]W. P. Su, J. R. Schrieffer, and A. J. Heeger, Proc. Natl. Acad. Sci. U.S.A. **77**, 5626 (1980); Phys. Rev. B **46**, 738 (1981).
[3]H. Takayama, Y. R. Lin-Liu, and K. Maki, Phys. Rev. B **21**, 2388 (1980).
[4]Y. Ono and A. Terai, J. Phys. Soc. Jpn. **59**, 2893 (1990).
[5]A. Terai and Y. Ono, J. Phys. Soc. Jpn. **60**, 196 (1991).
[6]K. Fesser, Phys. Rev. B **40**, 1962 (1989).
[7]D. Baeriswyl and K. Maki, Phys. Rev. B **38**, 8135 (1988).
[8]D. Baeriswyl and K. Maki, Phys. Rev. B **28**, 2068 (1983).
[9]H. A. Mizes and E. M. Conwell, Phys. Rev. B **43**, 9053 (1991).
[10]S. Stafström, Phys. Rev. B **43**, 9158 (1991).
[11]A. Terai and Y. Ono, J. Phys. Soc. Jpn. **55**, 213 (1986).
[12]Y. Ono, M. Kuwabara, and A. Terai (unpublished).
[13]A. Terai and Y. Ono, J. Phys. Soc. Jpn. **55**, 213 (1986).
[14]M. Kuwabara, Y. Ono, and A. Terai (unpublished).
[15]The quantity $1-Q(t)$ is analogous to the transition probability in a single-particle problem with two levels. Since we treat many particles in the present paper, $1-Q(t)$ may, in principle, be larger than unity or smaller than zero.
[16]In the third case, the simulation time is not enough, but there is an indication that the charge comes back to the chain 1.
[17]H. Kahlert, O. Leitner, and G. Leising, Synth. Met. **17**, 467 (1987).
[18]Z. Vardeny, J. Tanaka, H. Fujimoto, and M. Tanaka, Solid State Commun. **50**, 937 (1984).
[19]G. M. e Silva and Y. Wada, Synth. Met. **41-43**, 3713 (1991).